J. Fluid Mech. (1987), *vol.* 185, *pp.* 415–436
Printed in Great Britain

Sediment transport during unsteady settling in an inclined channel

By GUSTAV AMBERG AND ANDERS A. DAHLKILD
Department of Hydromechanics, The Royal Institute of Technology,
S-100 44 Stockholm, Sweden

(Received 1 April 1986 and in revised form 22 May 1987)

Settling of a dilute, monodisperse suspension between two inclined, narrowly spaced parallel plates is considered. Effects of sediment motion are accounted for. Lubrication theory and a simplified model for the particle motion lead to a system of two coupled nonlinear hyperbolic equations for the evolution of the two interfaces between clear fluid, suspension and sediment. Two problems are solved: batch settling and the filling of a channel that initially contains clear fluid. In the batch-settling case, the sediment has no major qualitative effect on the motion. In the filling problem, however, effects of sediment are important.

1. Introduction

Settling of a suspension in a tilted channel is a phenomenon that has attracted some attention during the last years. Detailed accounts of the history of the subject and its technological applications have been given by, among others, Acrivos & Herbolzheimer (1979), Davis & Acrivos (1985) and Amberg *et al.* (1986) to which the reader is referred for a complete exposition of the background to the present work. Here only a brief review of recent papers that are directly related to the problem will be given.

Acrivos & Herbolzheimer (1979) treated, both experimentally and theoretically, the time dependent settling of a suspension in a closed inclined vessel having an aspect ratio of order unity. In the parameter range considered, the clarified fluid forms a thin viscous boundary layer on the downward facing wall. The motion of the suspension outside this layer is slower and inertia dominated. In a later paper (Herbolzheimer & Acrivos 1981), the same problem is investigated for a narrow channel where the whole flow is viscously dominated.

In both these articles all effects of the particles that accumulate on the lower wall were neglected. It was assumed that, for the small concentrations considered, the sediment layer is sufficiently thin to be dynamically unimportant. It is the purpose of the present paper to include, in a simplified way, effects of the sediment in the analysis for a narrow channel.

Schneider (1982) investigated the Boycott effect in another parameter range where the force balance in both the clarified fluid and the suspension is between inertia and buoyancy. In this limit he was able to relax the assumption made in Acrivos & Herbolzheimer (1979) and Herbolzheimer & Acrivos (1981) that the concentration remains uniform. Concentration waves, of the same type as those found by Kynch (1952) in his classical study of vertical sedimentation could therefore be accounted for. Schneider considered time dependent settling in various vessels having inclined

walls and aspect ratios of order unity. The sediment was assumed to stick to upward facing walls and form a stationary layer of finite thickness.

Leung & Probstein (1983), Probstein & Hicks (1978) and Probstein, Yung & Hicks (1977) investigated time independent settling in a narrow inclined channel where a suspension is fed continuously at the top or bottom end. These authors considered essentially the same strong buoyancy limit as that studied by Herbolzheimer & Acrivos (1981). The sediment layer was taken into account and treated as a Newtonian fluid. Only steady processes were discussed. In their experiments, Probstein, Yung & Hicks remarked that the attainment of a steady state was cumbersome, since the response time of their experimental apparatus was of the order of one hour. Thus an understanding of the transient approach to steady state, which is attempted in this work, should be of practical importance even though the desired final state is steady.

In the present work, effects of sediment on some unsteady settling processes are considered. The same type of vessels and the same dynamical parameter range as considered by Herbolzheimer & Acrivos (1981) is treated. The paper can be seen as a unification and extension of the theories by Probstein & Hicks (1978) and Herbolzheimer & Acrivos.

The paper is planned as follows: In §2 the basic assumptions are stated and the basic equations given. A system of two nonlinear hyperbolic equations of first order for the evolution of the two interfaces between clear fluid, suspension and sediment is derived. Section 3 treats batch settling. The equations derived in §2 are solved numerically and the solutions discussed. In §4 the filling (with suspension) of a vessel that initially contains clear fluid is considered. Numerical solutions and an approximate solution for small-volume fractions are given. Section 5 contains some concluding remarks.

2. Formulation

The two-dimensional unsteady motion of a settling two-phase fluid will be considered. The fluid is contained between two parallel plates of length l, which are inclined at an angle α with the direction of gravity, see figure 1. The distance between the plates is $2h$ with $h \ll l$. The ends of the channel may be either closed or open. In the latter case, a net flux of suspension into the channel through the lower end is prescribed.

During the settling of the suspension, three distinct fluid layers form. A layer of clear fluid appears adjacent to the upper plate whereas a layer of sediment builds up at the bottom of the channel. The space between these two layers is occupied by suspension. The fluids in all three layers are assumed to behave as incompressible Newtonian fluids with constant (but different) properties†. This assumption may be reasonably well justified if the suspended particles are incompressible droplets with uniform radii, which coalesce into a continuous layer of fluid at the bottom plate.

If this description is to be realistic, a droplet is required to coalesce readily with the sediment layer at the suspension–sediment interface, but not with other droplets in the bulk of the suspension. The validity of this assumption is discussed in the Appendix.

† For the suspension, this means that the concentration of particles must be uniform. This matter is briefly discussed later.

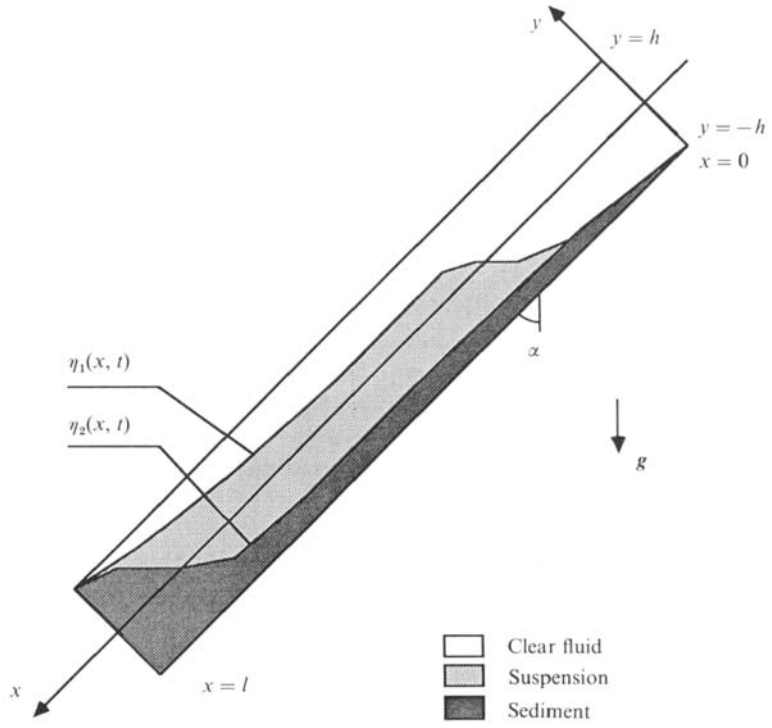

FIGURE 1. The geometry of the container.

Conversely, the particles may be assumed to be solid spheres. The suspension and the clear fluid can then be treated as Newtonian fluids (at least for moderate volume fractions up to approximately 20%), but it is not obvious that the sediment can be described by such a simple model. Probstein *et al.* (1977) and Leung & Probstein (1983) modelled sediment consisting of solid particles as a Newtonian fluid and found fair agreement with experiments. In the following we will primarily consider a suspension of droplets. The viscosities of the three layers can then be expected to be roughly the same if the viscosities of droplets and suspending liquid are approximately equal. The modifications necessary to treat the case where the viscosity of the sediment is much higher than that of the other two layers, as could be expected for a suspension of solid particles, will be discussed when appropriate.

The droplets or particles are assumed to have equal radii. The settling of polydisperse suspensions has been treated by Greenspan & Ungarish (1982), and Davis, Herbolzheimer & Acrives (1982), but this complication is not considered here. The bulk average of the velocity $\boldsymbol{u}$ of the suspension is given by the formula

$$\boldsymbol{u} = c\boldsymbol{u}_{\mathrm{d}} + (1-c)\,\boldsymbol{u}_{\mathrm{f}}. \tag{2.1}$$

Here c denotes the volume fraction of droplets, $\boldsymbol{u}_{\mathrm{d}}$ droplet velocity, and $\boldsymbol{u}_{\mathrm{f}}$ the velocity of the continuous fluid phase. For the settling velocity, i.e. the velocity of the droplets relative to the bulk average velocity of the suspension, the following empirical formula is used

$$\boldsymbol{u}_{\mathrm{d}} - \boldsymbol{u} = U_{\mathrm{s}} f(c)\,\boldsymbol{e}_g, \quad \boldsymbol{e}_g = \boldsymbol{g}/|\boldsymbol{g}|. \tag{2.2}$$

U_s is the settling velocity of a single droplet falling freely through quiescent fluid (see e.g. Batchelor 1967, p. 236):

$$U_s = ga^2 \frac{(\rho_d - \rho_f)}{3\mu_f} \frac{\mu_f + \mu_d}{\mu_f + \frac{3}{2}\mu_d}. \tag{2.3}$$

Here a denotes the droplet radius, μ viscosity and ρ density. Index d refers to the liquid in the dispersed droplets and index f to the suspending fluid. The formula (2.3) is accurate when the Reynolds number based on particle size ($2aU\rho_f/\mu_f$) is less than unity. In the derivation of (2.3), it is also assumed that the droplets are spherical. For a single droplet in quiescent fluid, this is true if the Reynolds numbers of the flow around and inside a droplet are small, or the surface tension is strong enough to keep the droplet spherical. In the presence of shear in the bulk flow, a finite surface tension is required to prevent rupture of the drop. Here we will assume that the droplet Reynolds number is small and that the surface tension is such that the droplets are spherical and (2.3) holds. In practice it is often observed that, due to surface impurities on the droplet surface, the sedimentation velocity of droplets follows Stokes law (equation (2.3) with $\mu_d/\mu_f = \infty$) instead of (2.3). Such effects are also disregarded here.

In (2.2), $f(c)$ denotes a non-dimensional function that accounts for particle interactions. $f(c) < f(0) = 1$ for $c > 0$ so that the average settling velocity is lower in a suspension of finite concentration than in a very dilute one. For a suspension of solid particles, a commonly used empirical correlation has been given by Richardson & Zaki (1954). Ishii & Chawla (1979) have given a relation that correlates sedimentation velocities in both droplet and solid-particle suspensions.

The equations of motion are made non-dimensional with the following scales:

time	$h/U_s f(c_0) \sin\alpha$
length in the x-direction	l
velocity in the x-direction	$lU_s f(c_0) \sin\alpha/h$
length in the y-direction	h
velocity in the y-direction	$U_s f(c_0) \sin\alpha$
pressure	$\mu U_s f(c_0) \sin\alpha\, l^2/h^3$
droplet volume fraction	c_0

The typical concentration c_0 is chosen as the initial value in the batch-settling case, or as the concentration of the feed in the problem where a net volume flux between the plates is considered. The latter case will henceforth be referred to as the filling problem.

In the cases to be studied in the present work, the parameter

$$\Lambda = \frac{gc_0(\rho_d - \rho_f) l^2}{\mu U_s f(c_0)}$$

is large, typically approximately 10^7. Λ is the ratio between a Grashof number and a sedimentation Reynolds number. The channel is assumed to be narrow in the sense that $h/l = O(\Lambda^{-\frac{1}{3}})$. Such cases are common in applications. The following additional non-dimensional parameters will appear

$$R = \frac{\rho_d l U_s f(c_0) \sin\alpha}{\mu},$$

$$\kappa = \frac{h}{l},$$

$$\beta = \frac{gc_0(\rho_d - \rho_f) h^3}{24\mu l U_s f(c_0) \tan\alpha} = \kappa^3 \Lambda \frac{1}{24 \tan\alpha},$$

R is a Reynolds number based on the length of the channel and the settling velocity. β is an estimate of the number of channel widths that a droplet is advected by the buoyancy-driven motion. As in Herbolzheimer & Acrivos (1981), the equations of motion will be considered in the limit

$$\kappa \to 0,$$
$$\kappa R \to 0,$$
$$\beta = O(1).$$

In the following we will take the viscosities of clear fluid, suspension and sediment to be the same. If the viscosities of the dispersed droplets and the continuous phase are equal, and if the droplets coalesce to a homogeneous film in the sediment layer, this is a fair approximation. The clarified layer and the coalesced sediment layer then have equal viscosities. The viscosity of the suspension is higher than that of the constituents. According to the correlation of Ishii & Chawla (1979), the suspension viscosity is 20 % higher than the continuous phase viscosity for 10 % volume fraction of droplets.

For a suspension of solid particles the sediment is more difficult to describe. Leung & Probstein (1983) and Probstein *et al.* (1977) described the sediment as a Newtonian fluid and found reasonable agreement with experiments. Probstein *et al.* reported an experimental value of 0.042 for the ratio of the viscosities of clear fluid and sediment. At 10 % volume fraction the viscosity in the bulk suspension is 30 % higher than the clear fluid viscosity according to the correlation of Ishii & Chawla. In order to minimize the number of free parameters and to formulate a simple model problem we have taken the viscosities to be equal in the three layers. In an investigation of a more detailed model for describing the motion of the three layers, Dahlkild has investigated effects of different viscosities. These results will be presented in a forthcoming paper. The effect of a more viscous sediment layer is discussed qualitatively here in connection to the solutions of the different flow cases.

With the assumption that the viscosities are equal in the three layers, the non-dimensional equations of motion can be written:

$$O(\kappa R) = -p_x + u_{yy} + 24\beta(\phi - 1), \tag{2.4a}$$

$$O(\kappa) = -p_y. \tag{2.4b}$$

Here $\phi = c/c_0$ is the scaled volume fraction of drops and u is the x-component of the bulk average velocity.

As both droplets and the continuous phase of the suspension are incompressible, the bulk velocity field is solenoidal, i.e.

$$u_x + v_y = 0. \tag{2.5}$$

The net volume flux is:

$$\int_{-1}^{1} u \, dy = Q = \frac{Q^*}{lU_s f(c_0) \sin \alpha}, \tag{2.6}$$

where Q^* is the prescribed dimensional volume flux per unit length in the lateral direction. In the batch case $Q = 0$ whereas in the filling problem $Q \sim 1$. The dimensional equation for the conservation of droplets reads:

$$c_t + \nabla \cdot (c\boldsymbol{u}_d) = 0.$$

Using (2.2) this may be written:

$$c_t + \{\boldsymbol{u} + \boldsymbol{e}_g U_s \frac{\mathrm{d}}{\mathrm{d}c}(cf(c))\} \cdot \nabla c = 0. \tag{2.7}$$

This equation implies that an unbounded, initially uniform suspension remains uniform. In the presence of boundaries, a continuous concentration variation may appear in the suspension adjacent to the sediment, if the initial concentration is sufficiently large (Kynch 1952; Schneider 1982). In the present work, it is assumed that concentration changes are discontinuous, i.e. the concentration in the suspension is constant ($= c_0$). The conditions that have to be imposed on the function $f(c)$ for this to be true are discussed in detail by Amberg *et al.* (1986).

In order to compute the motion of the settling suspension one needs, in addition to (2.4*a*,*b*) and (2.5), two equations for the positions of the interfaces

$$y = \eta_1(x,t) \quad \text{between clear fluid and suspension,}$$
$$y = \eta_2(x,t) \quad \text{between suspension and sediment.}$$

These equations are derived from the continuity of clarified liquid in the top layer and, likewise, continuity of sediment in the lower layer. Due to the sedimentation, clear fluid and sediment are produced at the upper and lower interfaces, respectively. This production must be balanced either by a flux gradient in the respective layer, or by a thickening of the layer. The derivation is discussed in more detail by Amberg *et al.* (1986). The result is:

$$\eta_{1t} - q_{1x} = -1, \tag{2.8a}$$

$$\eta_{2t} + q_{2x} = \epsilon, \quad \epsilon = \frac{c_0}{1-c_0}, \tag{2.8b}$$

where

$$q_1 = \int_{\eta_1}^{1} u \,\mathrm{d}y, \quad q_2 = \int_{-1}^{\eta_2} u \,\mathrm{d}y.$$

The fluxes q_1 and q_2 can be expressed as explicit functions of η_1 and η_2. This is done by calculating $u(y, \eta_1, \eta_2)$ from (2.4) in the regions

$$1 > y > \eta_1 \quad \text{with } \phi = 0,$$
$$\eta_1 > y > \eta_2 \quad \text{with } \phi = 1,$$
$$\eta_2 > y > -1 \quad \text{with } \phi = 1/c_0,$$

and determining the constants of integration from the flux condition (2.6) and the boundary conditions ($u = 0$ on $y = \pm 1$ and u, u_y continuous at $y = \eta_1, \eta_2$). After some algebra one finds

$$q_1 = -Qh(\eta_1) - \beta\left\{g(\eta_1) - \frac{1}{\epsilon}\kappa(\eta_1,\eta_2)\right\}, \tag{2.9a}$$

$$q_2 = -Qh(\eta_2) + \beta\left\{\frac{1}{\epsilon}g(\eta_2) - \kappa(\eta_1,\eta_2)\right\}, \tag{2.9b}$$

where

$$h(\eta) = -\tfrac{1}{4}(2+\eta)(1-\eta)^2, \tag{2.10}$$

$$g(\eta) = (1+\eta)^3(1-\eta)^3, \tag{2.11}$$

$$\kappa(\eta_1,\eta_2) = (1+\eta_2)^2(1-\eta_1)^2(3-(2+\eta_1)(2-\eta_2)). \tag{2.12}$$

The structure of the expressions (2.9*a*,*b*) for q_1 and q_2 should be noted. Effects of buoyancy enter only in the second terms whereas the first terms depend only on the imposed net volume flux between the plates or, which is equivalent, on the pressure drop between the open ends of the container.

In subsequent sections the system (2.8a,b) will be solved numerically and, in the filling problem, by a perturbation procedure. Boundary and initial conditions will be discussed separately for the cases considered.

3. Batch settling

In the batch-settling case the container is closed ($Q = 0$). Initially it is filled with a uniform suspension. Infinitesimal layers of clear liquid and sediment appear immediately at the top and bottom walls, cf. Kynch (1952). The initial condition for the solution η_1, η_2 of (2.8) is in this case

$$\begin{aligned} &\eta_1(x,0) = 1, \\ &\eta_2(x,0) = -1 \quad (0 < x < 1, \quad t = 0). \end{aligned} \tag{3.1}$$

As seen from (2.8), the rate of production of clear fluid per unit length is 1 and the rate of sediment deposition is ϵ. This means that no significant production of clear fluid or sediment can take place over the short end regions $x = O(\kappa)$ and $x = 1 - O(\kappa)$, where (2.8) is formally invalid. Thus, the volume fluxes of clear liquid, suspension and sediment must vanish separately at $x = 0, 1$. The formulae (2.9a,b) then imply that $\eta_1 = \pm 1$, $\eta_2 = \pm 1$ there. By analogy with the solution for the case where the sediment is neglected (Herbolzheimer & Acrivos 1981), it can be seen that the signs should be chosen as

$$\begin{aligned} &\eta_1(0,t) = \eta_2(0,t) = -1 \quad (x = 0, \quad t > 0), \\ &\eta_1(1,t) = \eta_2(1,t) = 1 \qquad (x = 1, \quad t > 0). \end{aligned} \tag{3.2}$$

Equation (2.8), with the initial condition (3.1) and the boundary condition (3.2), appear to define a well-posed hyperbolic problem. It was solved numerically using the scheme given by Roe (1981).

A disturbing property of the system (2.8a,b) is that, for certain combinations of values of η_1 and η_2, the characteristic velocities of the system are complex. The problem is consequently ill-posed. The physical reason for this troublesome state of affairs is that the stratified quasi-parallel three-layer flow in the container is linearly unstable for wavelike disturbances of infinite wavelength. However, even if the system (2.8) is formally ill-posed, the consequences are not very serious due to two circumstances. Firstly, the regions in the (η_1, η_2)-plane where the characteristics are complex are small, see figure 2. Secondly, the growth rate for unstable disturbances can be shown to be small, typically less than 0.1. In general, the motion will therefore be subject to a weak instability during a small time interval. The net effect of the instability can thus, on reasonable grounds, be expected to be small. In the numerical computations the characteristic roots of the system (2.8) were slightly adjusted to real values in the unstable regions shown in figure 2. Numerical experiments with different schemes for adjustment showed very small differences in the solution.

A more satisfactory way of eliminating the difficulties associated with complex characteristics would be to include weak diffusive effects in (2.8) as outlined in Amberg *et al.* (1986) (the text preceding equation (2.33)). This leads to a well-posed parabolic problem. Work on this problem is in progress and preliminary results confirm the results obtained by the *ad hoc* method used here.

Figure 3 shows a numerical solution with the parameter setting $c_0 = 0.01$ and $\beta = 0.25$. The sequence of graphs shows the shapes of the layers of clear fluid (white), suspension (grey) and sediment (black) at different times. The timescale is such that a particle would fall across the channel in two time units in the absence of buoyancy-

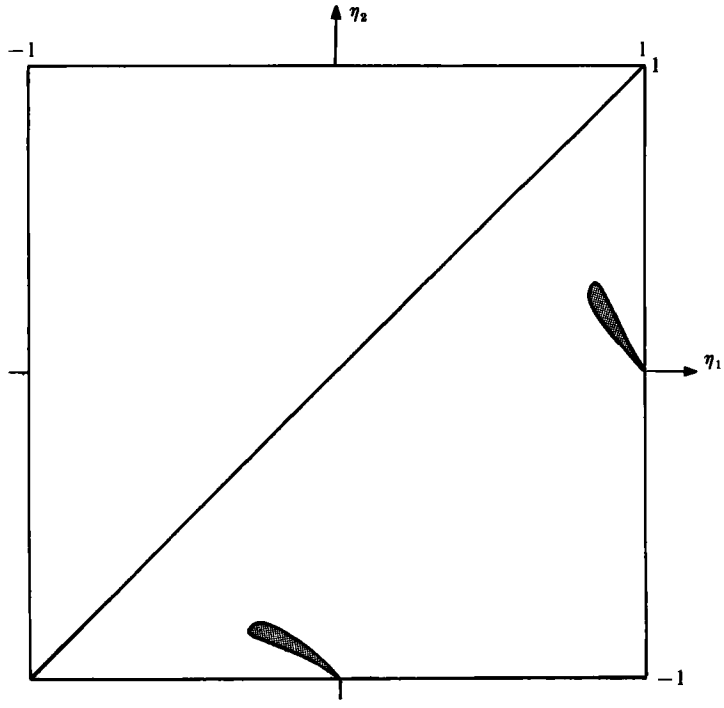

FIGURE 2. The (η_1, η_2)-plane shown for the parameter values $Q = 0$, $\epsilon = 1$. The shaded areas mark regions where the characteristic velocities are complex.

driven motion of the bulk. It should be noted that the channel width is exaggerated in figures 3, 4, 6, 7 and 8. A true width to length ratio is $\kappa = 0.01$ typically. The lubrication theory approximations made in §2 mean that variations of lengthscale $O(\kappa)$ in the solution are not resolved. A discontinuity (shock) of η_1, as shown in figure 3, is thus a model for a finite variation of η_1 over a short distance of order κ in the x-direction.

In the batch case the parameter β may be interpreted as a lengthscale. This may be seen from (2.8) with $Q = 0$, from which β may be removed by introducing x/β as a new length variable. For the two-layer case it may also be inferred from the corresponding equation, i.e. (2.8a) with $\eta_2 = -1$, that β is the maximum non-dimensional distance over which the lower end is felt (Amberg *et al.* (1986). With effects of sediment this is only approximately true.

The process shown in figure 3 starts at time $t = 0$ (not shown) when the entire container is filled with a suspension of uniform concentration. At time 0.4 a layer of light, clear fluid flowing upwards (to the right in figure 3) has formed beneath the downward facing wall. A very thin layer of sediment has accumulated on the upward facing lower wall and flows very slowly downwards (to the left). For the small concentration considered, the layer of sediment is hardly visible in the graphs. At $t = 0.8$ the clear layer has grown thicker. Some distance away from the ends the interface between clear fluid and suspension is parallel to the walls and moves with constant velocity towards the lower wall. At the upper end, a shock propagating downwards is formed immediately. Above this shock the clear fluid that flows upwards beneath the downward facing wall is collected. There is also a small,

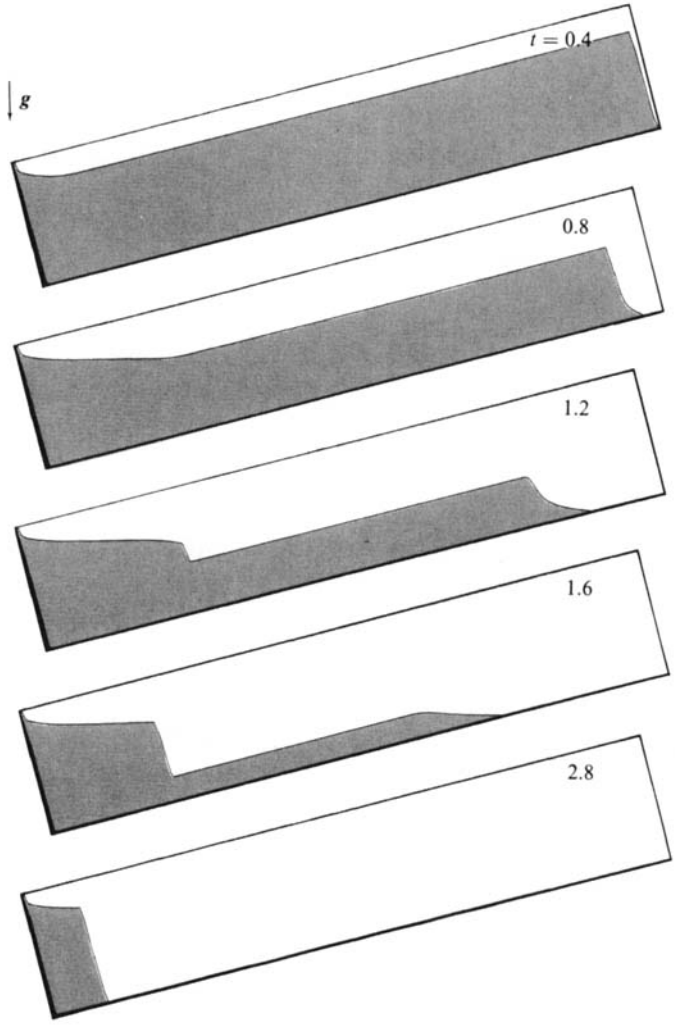

FIGURE 3. Numerical solution for the batch case shown at times $t = 0.4$, 0.8, 1.2, 1.6, 2.8. The parameter setting is $c_0 = 0.01$, $\beta = 0.25$, $Q = 0$.

approximately triangular region of suspension left above it. This region increases in length and height until $t = 1.6$ when the shock disappears.

Near the lower end the interface between clear fluid and suspension attains, to lowest order in c_0, a steady shape, which increases in length until $t = 1$. In the case shown in figure 3, the maximum length of the almost steady part of the interface is very close to $\beta = 0.25$. For $t > 1$ a shock appears which grows in strength and propagates downwards. At $t = 2$ the straight part of the interface outside the end regions reaches the lower wall. A more detailed discussion of this scenario is given by Herbolzheimer & Acrivos (1981). After time $t = 2$, most of the channel contains only clear fluid and a thin film of sediment on the upward facing wall. This film is slowly seeping downwards, its thickness approaching zero asymptotically. The timescale for this motion is $O(1/\epsilon)$.

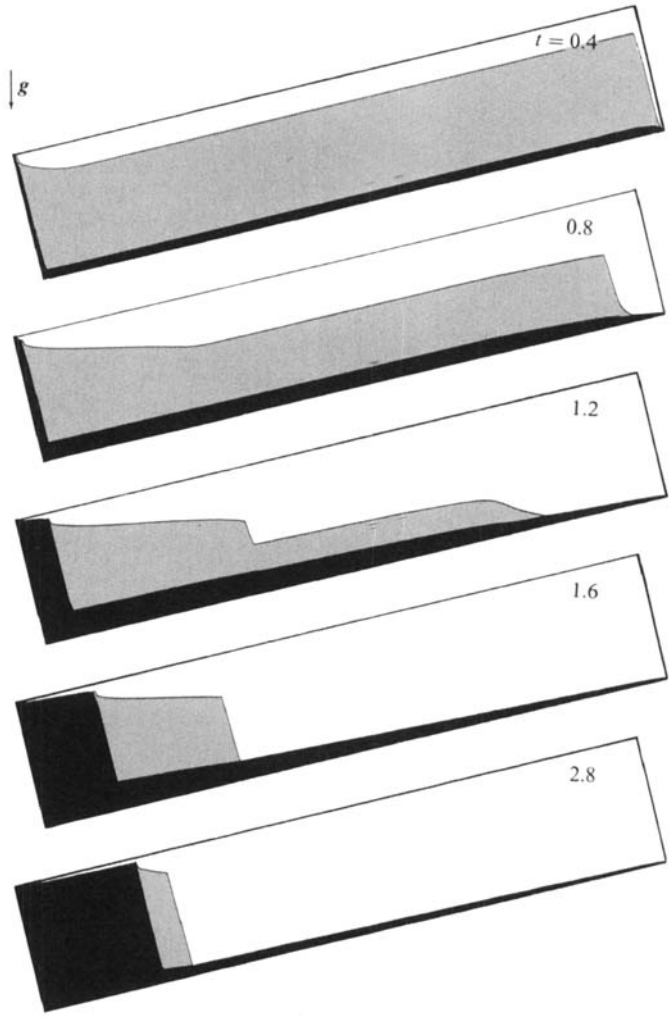

FIGURE 4. Numerical solution for the batch case with larger effects of sediment. The parameters are $c_0 = 0.24$, $\beta = 0.25$, $Q = 0$.

At the low concentration in figure 3, the sediment is, of course, hardly visible at all in the graphs, and has a negligible dynamical effect. The numerical solution agrees very well with the analytical solution given by Herbolzheimer & Acrivos (1981), who neglected the sediment, except for one discrepancy. The difference concerns the finite region of suspension left behind the upper shock. This matter is discussed in some detail by Amberg *et al.* (1986), who corrected the solution given by Herbolzheimer & Acrivos in this respect. The present numerical solution of the three-layer problem agrees excellently with the analytical solution of the two-layer problem given by Amberg *et al.* (1986).

Figure 4 shows a case where the sediment cannot be neglected ($c_0 = 0.24$). The value of β ($= 0.25$) is the same as in figure 3, i.e. the ratio between the buoyancy-driven velocity and the settling velocity is approximately the same. One may say that there are two additional effects caused by the presence of a finite amount of

sediment. Firstly, the motion of the sediment will be appreciable, which means that the shear stress at the interface between sediment and suspension will tend to drag the suspension towards the lower end of the container. Secondly, the growing thickness of the layer of sediment will squeeze the clear fluid and suspension towards the downward facing wall.

It can be seen from figure 4 that the principal features of the process are quite similar to those shown in figure 3. Near the lower end, the shape of the clear fluid–suspension interface is now only approximately steady due to the additional effects mentioned above. Also, the accumulated sediment at the lower end acts as a moving boundary so that the quasi-steady shape is displaced upwards. Outside the end regions, there is also some distortion of the clear fluid–suspension interface compared to the case shown in figure 3. This distortion is caused by a viscously dominated gravity wave, which is propagating downwards from the upper end on the suspension–sediment interface. Another effect is that the growing thickness of the sediment layer shortens the path of fall of the droplets on the clear fluid–suspension interface and thus reduces the non-dimensional time for settling outside the end regions.

The two shocks that appear in the case shown in figure 3 have counterparts in figure 4. The general behaviour of these shocks is quite similar in the two cases. In figure 4 however, an additional shock appears due to the accumulation of sediment in the lower end of the container.

In a case where the sediment is much more viscous than the clear fluid and the suspension, the process is somewhat different. The most important effect is that the flux in the sediment layer is decreased, i.e. the sediment flows down the lower plate more slowly. In the limit of a very viscous sediment, the suspension first settles into an almost stationary sediment layer of uniform thickness (in a time ≈ 2). During this time the sediment layer is felt only through the decreasing width of the space occupied by suspension and clear fluid. The sediment layer then flows slowly down the inclined plate to the lower end of the channel. The timescale of this motion can be shown to be $\mu_s/(\mu_f \cdot \beta c_0(1-c_0))$ (μ_s = effective sediment viscosity, μ_f = clear fluid viscosity). This is analogous to the case with equal viscosities in all three layers and a very low volume fraction c_0 that was discussed above ($c_0 \ll 1$, $\mu_s = \mu_f$, $\beta = O(1)$), where the time required for the sediment to reach the lower end is of order $1/\epsilon \approx 1/c_0$.

4. The filling problem

In this section, a container with open ends and a prescribed net volume flux $Q \neq 0$ between the plates at $y = \pm 1$ is considered. At time $t = 0$, the container is filled with clear fluid and suspension of uniform concentration c_0 is pumped into the container at the lower end. The volumetric flux $Q < 0$ at $x = 1$ is assumed to be constant and the transient motion of the suspension that enters the container will be computed. The corresponding problem in cases where the sediment can be neglected has been treated by Amberg *et al.* (1986, §4). The appropriate initial condition is

$$\eta_1(x, 0) = \eta_2(x, 0) = -1 \quad (0 < x < 1). \tag{4.1}$$

The formulation of boundary conditions at $x = 0, 1$ is not trivial and requires some consideration. By assumption, no clear fluid or sediment enters the container at $x = 1$. However, the sediment that after some time has settled in $x < 1$ may well flow

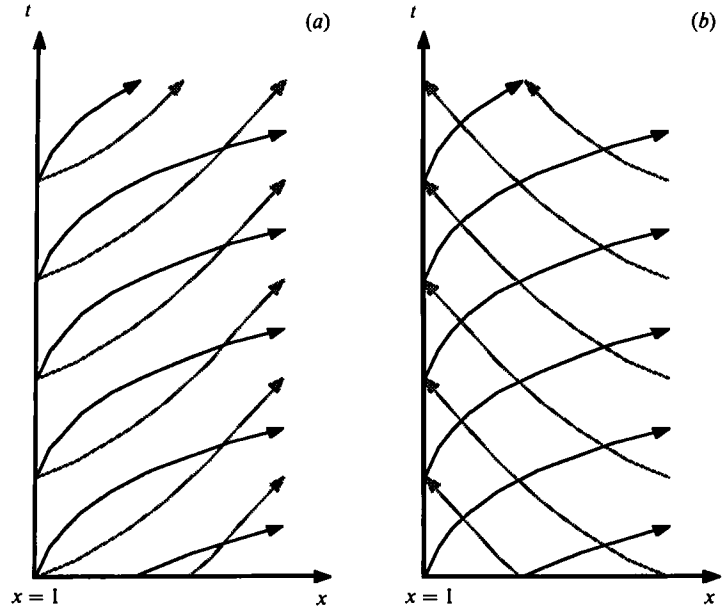

FIGURE 5. Schematic sketch of the characteristics in the immediate vicinity of the inlet, $x = 1$, for two cases where: (*a*) both η_1 and η_2 should be prescribed at $x = 1$, (*b*) only η_1 should be prescribed at $x = 1$. Characteristics of ——, the A-family; ..... the B-family.

downwards and leave† the container at $x = 1$. Another possibility is that all sediment leaves the container at $x = 0$. In the former case, the location of the interface between sediment and suspension at $x = 1$ depends on the solution in $x < 1$ and can obviously not be prescribed. In the latter case, one obviously has $\eta_2(1, t) = -1$. The number of boundary conditions that can be prescribed at $x = 1$ thus depends on the solution. More precisely, if both characteristics of the system (2.8) for a given value of t are running into the region $x < 1$ from $x = 1$, two boundary conditions must be prescribed at this value of x. Figure 5(*a*) shows schematically the characteristics in the immediate vicinity of the inlet for such a case. This situation always prevails initially. On the other hand, if only one characteristic enters $x < 1$ from $x = 1$ for a given value of t, only one boundary condition can be prescribed at $x = 1$. In certain cases this may occur after a finite time and a typical case is shown in figure 5(*b*).

In all cases considered in this work, both characteristics are at $x = 0$ running out from the region $x > 0$. No boundary condition can therefore be prescribed at $x = 0$.

In summary, the following boundary conditions are prescribed:

$$\eta_1(1, t) = 1, \quad \eta_2(1, t) = -1, \tag{4.2}$$

where the second condition has to be omitted if only one characteristic enters the region $x < 1$ at $x = 1$. No boundary condition is specified at $x = 0$.

Note that the use of the lubrication approximation, which yields the flux expressions (2.9), has also reduced the number of boundary conditions that are possible to impose on the flow. With the full Navier–Stokes equations, the velocities and the interface positions would be specified independently at inlet and outlet. Rubinstein (1980) analysed this problem and found that for small Reynolds

† Note that this flux of sediment is included in Q.

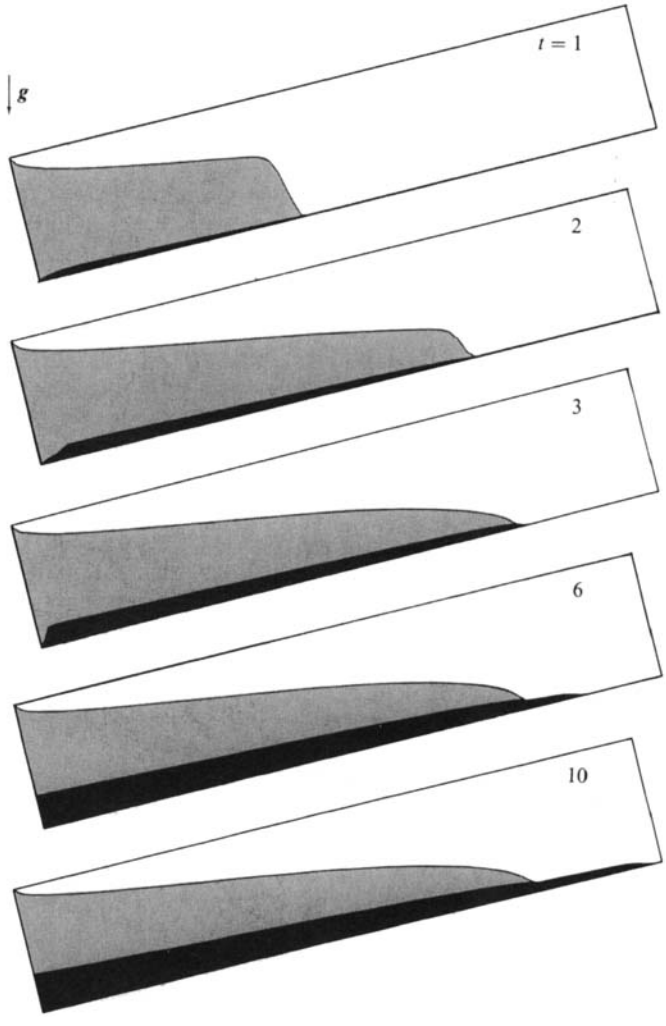

FIGURE 6. Numerical solution for the filling problem shown at times $t = 1, 2, 3, 6, 10$. The parameter setting, $c_0 = 0.091$, $\beta = \frac{1}{24}$, $Q = 0.8$, is such that the sediment leaves the container at $x = 1$.

numbers, the thickness of the layers are quickly adjusted (within a length approximately equal to the channel width) to those given by the fluxes (2.9) according to lubrication theory. Thus, if the inlet or outlet is constructed so that the layer thicknesses are not compatible with (2.9), Rubinstein's analysis shows that the resulting distortion of the interface can extend at most a distance approximately equal to the channel width into the channel. Beyond that position, the relations (2.9) between layer thicknesses and fluxes hold.

The filling problem considered in this section was solved numerically using the scheme† given by Engquist & Osher (1981). An analytical solution obtained by perturbation methods will be given later in this section. At each timestep, the

† The Engquist–Osher scheme turned out to require excessive amounts of computer time for the batch-settling problem treated in the previous section. The numerical solution of that problem therefore had to be reconsidered by using Roe's scheme.

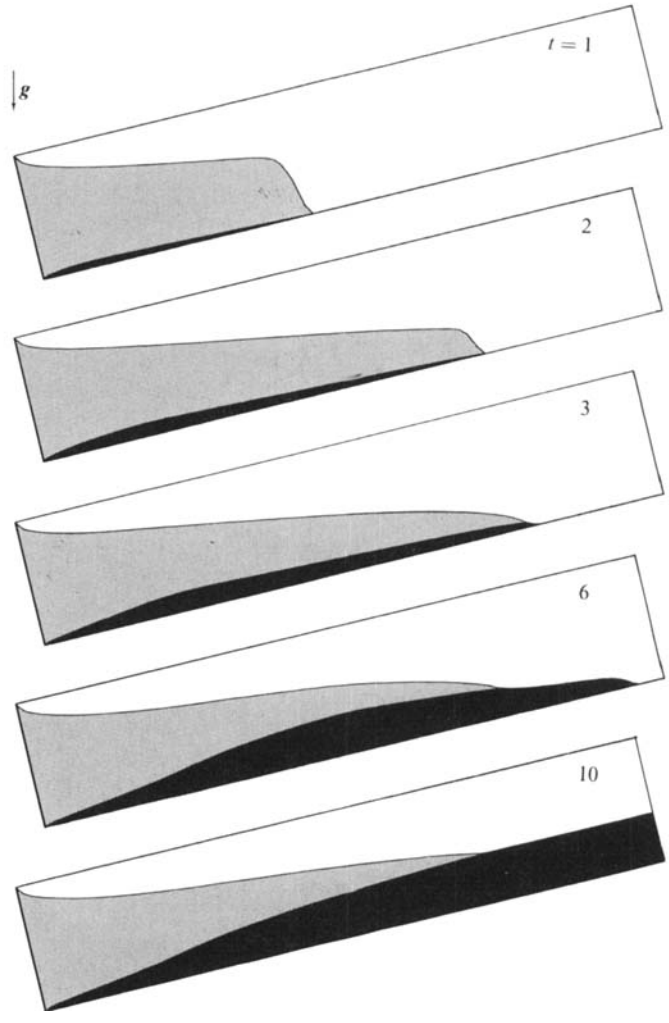

FIGURE 7. Numerical solution for the filling problem in a case where the sediment goes out at $x = 0$. The parameter setting is $c_0 = 0.091$, $\beta = \frac{1}{48}$, $Q = 0.8$.

direction of the characteristics at $x = 1$ was computed in order to determine the correct number of boundary conditions to be imposed at $x = 1$. In the case when only one boundary condition is imposed at $x = 1$, the scheme is such that, in order to compute the solution at time $t+\Delta t$, the value of η_2 at a fictitious point just outside the lower end is needed at time t. This value is obtained from the solution in $x \leqslant 1$ by taking $\eta_1 = 1$ and discretizing (2.8*b*) with one-sided differences.

Figure 6 shows the evolution to a steady state for the parameter values $\epsilon = 0.1$, $\beta = \frac{1}{24}$ and $Q = -0.8$. The numerical value of $|Q|$ is an estimate of the length l_s of the region occupied by suspension in the steady state (cf. Amberg *et al.* 1986, §4). For the case shown in figure 6 this estimate of l_s is quite accurate at $t = 10$, when the clear fluid–suspension interface is steady and almost all sediment leaves the channel at the lower end. For the opposite case, where no sediment emerges at the lower end as shown in figure 7, one has instead $l_s \approx |Q|\ (1-c_0)$. The value of β is significantly

smaller than in the batch-settling case considered in the previous section which implies that the difference in density between clear fluid and suspension is here of minor importance. Buoyancy effects will only appear because the sediment is significantly heavier than the clear fluid and the suspension.

The sequence shown in figure 6 indicates that the approach to a steady state occurs on two timescales. The interface between clear fluid and suspension is approximately steady for $t \geqslant 3$. The sediment layer however, continues to grow for considerable time and is not steady until $t > 10$. In the first three graphs, no sediment is leaving the channel and both boundary conditions (4.2) are imposed. However, at time $t = 3$ a shock has appeared on the interface between suspension and sediment. (The corresponding discontinuity on the other interface is too weak to be seen in the graphs.) This shock, which is a consequence of downward flow of heavy sediment, propagates downwards. After the inlet $x = 1$ is reached, one of the characteristic velocities changes sign and runs out from the region $x < 1$. Thus, only one boundary condition can be imposed at $x = 1$ for subsequent times. In this case effects of buoyancy eventually become sufficiently strong for the main part of the sediment to leave the container at the inlet. It can be shown that, after sufficiently long time, there is also a very small flux of sediment through the outlet.

Figure 7 shows a case where the geometry of the channel and the values of c_0 are the same as in figure 6 but the value of β is decreased by a factor of a half, i.e. $\beta = \frac{1}{48}$ in figure 7. Initially, the flow is very similar to that shown in figure 6. However, because buoyancy effects are weaker in this case, the shock on the lower interface does not appear. The layer of sediment never becomes sufficiently heavy to slide downwards to the inlet but leaves the container at the outlet. Also in this case, two timescales govern the approach to the steady state.

For a case with a very viscous sediment, such as in the sedimentation of a particulate suspension, the tendency of the sediment to be washed upwards is increased. As discussed in the text following (2.12), the sediment flux can be viewed as composed of one part due to the density differences and another due to the imposed volume flux through the channel. For a fairly thin and very viscous sediment layer, simple estimates show that the buoyancy induced flux is approximately $\beta/(\epsilon m)$, where $m = \mu_s/\mu_f$, and the flux due to the imposed pressure gradient is approximately Q/m. Thus the relative importance of buoyancy *vs.* imposed pressure gradient would appear to be unchanged by an increased sediment viscosity. However, with increasing sediment viscosity, the sediment layer must grow thicker to carry the same flux. When the thickness of the layer increases, the imposed flux can increase up to the net flux Q in the channel, but the magnitude of the buoyancy induced part is unchanged, approximately $\beta/(\epsilon m)$. Thus, with increasing m and a sufficiently thick sediment layer, the downward buoyancy flux decreases, while the upward imposed flux can always accommodate the required sediment flux.

Leung & Probstein (1983) have calculated the steady sedimentation in a continuously fed inclined container, using a three-layer model with a viscous sediment layer. They studied cases with fairly strong buoyancy, corresponding to $\beta > 0.3$. Here β has been chosen considerably smaller. For the comparatively large values of β used by Leung & Probstein, buoyancy is strong enough to make the sediment go out at the lower inlet end, despite the fact that the sediment is very viscous.

The presence of two timescales which was noted in the discussion of figure 6, may be used to construct an approximate analytical solution as a perturbation expansion

in the small parameter $\epsilon = c_0/(1-c_0)$. It is seen from (2.8b) that only an $O(\epsilon)$ amount of sediment is produced per unit length during times of order unity. The sediment layer is then at most $O(\epsilon)$ thick, i.e. $\eta_2 = -1+O(\epsilon)$. Thus (2.9b) shows that the sediment flux function q_2 is $O(\epsilon^2)$. New $O(1)$ variables φ_2, η_2 are defined as:

$$q_2 = \epsilon^2 \varphi_2, \quad \eta_2 = -1+\epsilon\eta_2. \tag{4.3a,b}$$

Introducing these into (2.8) one finds:

$$\eta_{1t} - q_{1x} = -1, \quad \eta_{2t} + \epsilon\varphi_{2x} = 1. \tag{4.4a,b}$$

From (4.4b) it is evident that η_2 cannot be stationary on this timescale, since the main balance is between η_{2t} and the source term on the right-hand side.

Non-dimensional times of order one, for which (4.4) are valid, represent the shorter of the two timescales in the problem. The longer timescale is the time required for η_2 to reach an approximately steady state. As seen from figures 6 and 7 there are two qualitatively different steady states. In the flow in figure 6 all the sediment comes out at the bottom inlet end, while in figure 7 the sediment leaves the channel at the top outlet. Which of the two cases actually occurs is determined by the relative magnitudes of ϵ and β. In the steady state the balance in equation (2.8b) is between q_{2x} and ϵ. By considering the expression for q_2 in (2.9b), it can be shown that the situation in figure 6 prevails if $\beta \gg \epsilon^{\frac{1}{3}}$, or more accurately $\beta \gg \epsilon^{\frac{1}{3}}(\frac{3}{4}|Q|)^{\frac{2}{3}}/8$. In the opposite case, $\beta \ll \epsilon^{\frac{1}{3}}(\frac{3}{4}|Q|)^{\frac{2}{3}}/8$, the case in figure 7 occurs. In the intermediate range, $\beta \approx \epsilon^{\frac{1}{3}}(\frac{3}{4}|Q|)^{\frac{2}{3}}/8$, it is possible to adjust the parameters so that there is a significant efflux of sediment at both ends. Note that consistency with the approximations made in §2 require that $\beta, \epsilon \gg \kappa$.

In the remainder of this section, attention is restricted to cases of the type in figure 6. It is therefore assumed that $\beta = O(1)$ and $\epsilon \ll 1$. For this case the time to establish a steady state may be estimated to be $O(\epsilon^{-\frac{1}{3}})$. The thickness of the sediment layer is then $O(\epsilon^{\frac{2}{3}})$.

It is assumed that the dependent variables possess expansions in ϵ of the following form on the short timescale:

$$\eta_1 = \eta_1^0 + \epsilon\eta_1^1 + O(\epsilon^2), \quad \eta_2 = \eta_2^0 + \epsilon\eta_2^1 + O(\epsilon^2), \tag{4.5a,b}$$

$$q_1 = q_1^0 + \epsilon q_1^1 + O(\epsilon^2), \quad \varphi_2 = \varphi_2^0 + O(\epsilon), \tag{4.5c,d}$$

where
$$q_1^0 = \tfrac{1}{4}Q(2+\eta_1^0)(1-\eta_1^0)^2 - \beta(1-\eta_1^0)^3(1+\eta_1^0)^3,$$
$$q_1^1 = \eta_1^1[-\tfrac{3}{4}Q(1-(\eta_1^0)^2) + 6\beta\eta_1^0(1-\eta_1^0)^2(1+\eta_1^0)^2] - 3\beta(\eta_2^0)^2(1-\eta_1^0)^2(1+\eta_1^0),$$
$$\varphi_2^0 = \tfrac{3}{4}Q(\eta_2^0)^2 + 8\beta(\eta_2^0)^3 + 3\beta(\eta_2^0)^2(1-\eta_2^0)^2(1+\eta_1^0).$$

The system (4.4) is written in characteristic form and the expansions (4.5) are introduced. This yields expressions for η_1 and η_2 along the characteristic curves of the system. For this system of two unknowns there are two families of characteristic curves, labelled the A- and the B-family. The shapes of these curves are obtained as expansions in ϵ according to:

$$x_{\mathrm{A}} = x_{\mathrm{A}}^0 + \epsilon x_{\mathrm{A}}^1 + O(\epsilon^2), \quad x_{\mathrm{B}} = x_{\mathrm{B}}^0 + \epsilon x_{\mathrm{B}}^1 + O(\epsilon^2). \tag{4.6a,b}$$

Here $x_{\mathrm{A}}^0 \ldots x_{\mathrm{B}}^1$ as well as $\eta_1^0 \ldots \eta_2^1$ and time are functions of the parameters a (along an A-characteristic) and b (along a B-characteristic).

The procedure for solving (4.4) by the expansions (4.5), (4.6) is lengthy and not trivial. For the sake of brevity and clarity, it is omitted here. The details of this

calculation will be presented elsewhere. However, to bring about a greater qualitative understanding of the filling process, the result is given.

The solution is obtained in implicit form. The unknowns η_1, η_2 are calculated as functions of a, b along with x_A, x_B. Substitution of the expansions (4.5), (4.6) into the equations on characteristic form gives that η_1 is determined, within an error $O(\epsilon^2)$, along a characteristic of the A-family, i.e. as a function of a alone. Similarly η_2 is determined on B-characteristics, as a function of b alone. The solution for η_1 is, expressed in this form:

$$\eta_1(a) = \eta_{1i}^0 - a + \epsilon\left(\eta_{1i}^1 + \int_0^a q_{12}^1 \frac{\partial \eta_2^0}{\partial x}(x_A^0, t)\,\mathrm{d}a\right) + O(\epsilon^2), \tag{4.7a}$$

along the curve

$$x_A(a) = x_{Ai}^0 - q_{1i}^0 + q_{1i}^0 - \epsilon(q_{1i}^1 - q_{1i}^1 + x_{Ai}^1) + O(\epsilon^2), \tag{4.7b}$$

$$t(a) = t_{Ai} + a. \tag{4.7c}$$

The solution for η_2:

$$\eta_2(b) = \eta_{2i}^0 + b + \epsilon\left(\eta_{2i}^1 - \int_0^b \frac{q_{21}^0}{q_{11}^0}\,\mathrm{d}b\right) + O(\epsilon^2), \tag{4.8a}$$

$$x_B(b) = x_{1i}^0 + \epsilon(\varphi_2^0 - \varphi_{2i}^0 + x_{Bi}^1) + O(\epsilon^2), \tag{4.8b}$$

$$t(b) = t_{Bi} + b; \tag{4.8c}$$

here

$$q_{21}^0 = -3\beta(\eta_2^0)^2(1-\eta_1^0)(1+3\eta_1^0),$$

$$q_{11}^0 = -\tfrac{3}{4}Q(1-(\eta_1^0)^2) + 6\beta\eta_1^0(1-\eta_1^0)^2(1+\eta_1^0)^2,$$

$$q_{12}^1 = -6\beta\eta_2^0(1-\eta_1^0)^2(1+\eta_1^0).$$

The indices i denote initial values. These are obtained from the boundary and initial conditions (4.1), (4.2). To plot the solution, η_1 say, as a function of x at a certain instant, the parameter a is expressed in t and eliminated from (4.7). The interface is then obtained as a function of x at the chosen instant by plotting η_1 versus x_A for different initial positions t_{Ai}, x_{Ai} of the characteristic curve. As the initial position is varied over the boundary of the (x,t)-plane, (η_1, x_A) is a parametric representation of the interface shape.

As seen from the numerical calculations the solutions contain shocks. These must be inserted whenever a characteristic from one of the two families intersects another curve of the same family. As remarked above, η_1 is determined along A-characteristics and η_2 along B-characteristics to this order of approximation. Thus when two curves from the A-family (say) intersect, a discontinuity in η_1 is inserted. Since η_2 is not affected by the A-characteristics to this order, no discontinuity is required in η_2. The speed of the η_1-discontinuity is then determined by conservation of clear fluid (or sediment if the shock is in η_2) over the discontinuity, just as in classical kinematic wave theory (see e.g. Amberg *et al.* 1986). Thus an ordinary differential equation (involving the solutions (4.7), (4.8)) can be formulated for the position of the shock and solved numerically.

In figure 8 the interfaces obtained in this manner are shown for a case with $Q = -0.8$, $\beta = \frac{1}{24}$, $\epsilon = 0.1$ at two times, $t = 2, 10$. The dashed curves in the same graph show the result of a numerical calculation. The agreement is satisfactory.

Figure 9 shows the two families of characteristic curves (x_A, x_B) in an x versus $t\epsilon^{\frac{1}{3}}$ diagram on the long timescale. Curves of the A-family, corresponding to the evolution of η_1, enter from the inlet at $x = 1$ and move rapidly up the channel (to the right). When plotted on the long timescale the A-characteristics are almost parallel to the x-axis.

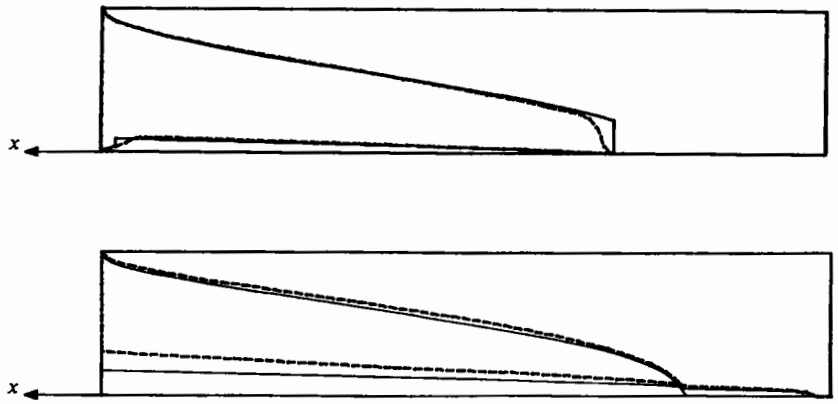

FIGURE 8. Comparison between —, the analytical solution and – – –, the numerical for a case with $c_0 = 0.091$, $\beta = \frac{1}{24}$, $Q = 0.8$. Time is $t = 2.0$ in the upper graph and $t = 10.0$ in the lower.

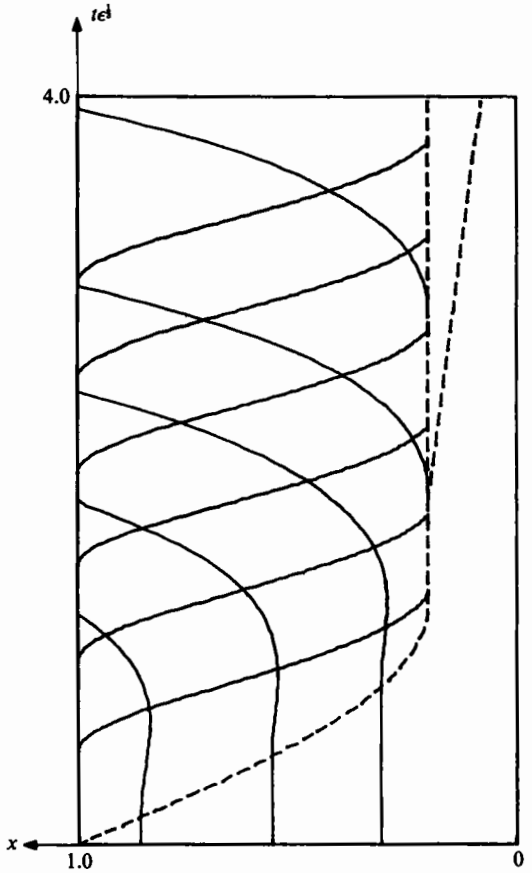

FIGURE 9. The characteristic curves on the long timescale $t \cdot \epsilon^{-\frac{1}{4}}$ for $c_0 = 0.091$, $\beta = \frac{1}{24}$, $Q = -0.8$. The A-family of characteristics is deflected to the right and the B-family to the left.

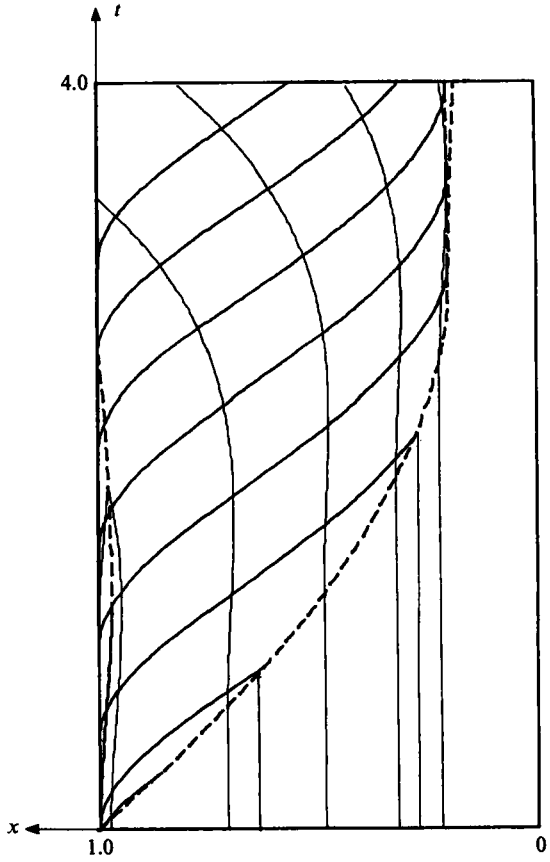

FIGURE 10. The characteristic curves on the short timescale for $c_0 = 0.091$, $\beta = \frac{1}{24}$, $Q = -0.8$. The A-family is deflected to the right and the B-family to the left.

Characteristics of the B-family, related to the evolution of the sediment layer, originate on the x-axis. When the initial shock (the upper end of the suspension region propagating up the channel initially) has passed, these characteristics are deflected down towards the outlet (to the left). When viewed on the long timescale the shock formally passes through the channel instantaneously.

In figure 10 the characteristics are shown on the short timescale. Due to the boundary condition $\eta_1 = 1$ at $x = 1$. there are A-family characteristics starting on the t-axis running up into the channel. The initial condition $\eta_1 = -1$, is propagated along the straight characteristics starting at $t = 0$. A shock is formed at $x = 1$, $t = 0$ when the A-characteristics starting at $x = 1$ intersect the straight characteristics carrying the initial value. This shock propagates up the channel until its strength has decayed to zero at $t = 2.88$.

In figure 10 the B-characteristics carry the initial condition $\eta_2 = -1$ straight up, across the shock path starting at $x = 1$, $t = 0$. When this shock has passed, the sediment layer starts to build up and the B-characteristics first make a slight bend upwards (to the right) and are then deflected down towards the inlet. Due to the slight bend upwards, the rightmost B-characteristic will become tangent to the initial shock at a certain instant. At $x = 1$, the boundary condition $\eta_2 = -1$ will initially cause B-characteristics to enter the channel from the inlet. At $t = -Q/(16\beta)$

these characteristics intersect and a shock is formed a small distance in from $x = 1$. This shock moves down and leaves the channel at $t = 2.56$ for the parameter values in figure 8. From this instant on, the B-characteristics leave the region at $x = 1$ and $\eta_2 \neq -1$ there.

This shock is the same as the one observed in the discussion of the numerical results. The time $t = 2.56$ is when the boundary condition (4.2) is switched from prescribing both η_1 and η_2 at $x = 1$ to prescribing only η_1.

5. Conclusions

Effects of sediment on the time dependent gravity settling of a suspension in a narrow inclined container has been studied. Two cases were investigated. In batch settling, where the container is closed and is initially filled with a suspension of uniform concentration, the sediment has only a minor qualitative effect on the flow. The thickness of the sediment layer is always $\leqslant O(c_0)$. The evolution of the regions occupied by suspension and clarified liquid are qualitatively similar to those obtained when the sediment is neglected. One additional region is present at the bottom end, where the sediment is eventually collected. Also an additional shock appears.

The second problem considered is the filling (with suspension) of an open channel that initially contains clear fluid. The suspension enters the channel at the lower end. In this problem two timescales appear. For times of order unity, the suspension reaches over most of the channel length and the interface between suspension and clear fluid is approximately steady. On this time scale, the sediment layer is thin, $\leqslant O(c_0)$. The sediment layer grows on the $O(1)$ timescale and reaches its steady state on a timescale $O(c_0^{-\frac{1}{3}})$. In the steady state, the thickness of the sediment layer is $O(c_0^{\frac{2}{3}})$.

Depending on the relative importance of buoyancy and imposed flow rate, the sediment may leave the channel at either the inlet or the outlet (or both). If buoyancy is important, as it will be for instance in a wide enough channel, the flow in the heavy sediment layer is directed downwards, opposite to the imposed net flux. The sediment will leave the channel at the inlet. However, if the density difference is less important, as it would be in a slightly narrower channel, the imposed flow is sufficient to drag the sediment upwards at all times. The sediment then leaves the channel at the outlet. The former possibility appears if $\beta \gg \epsilon^{\frac{1}{2}}$ and the latter if the opposite is true.

A complication of the mathematical model is that the characteristic velocities of the system of hyperbolic equations for the interfaces are complex for certain combinations of interface positions. This is due to the presence of a weak instability for long wavelengths. The growth rate of this instability is small. Also, unstable combinations of interface positions occur only rarely. It is therefore judged that the flow is still described reasonably well by the hyperbolic system that was used.

We are greatly indebted to Professor Fritz Bark for continuous guidance in the course of this work, to Professor Bertil Gustavsson for valuable advice on the numerics and to Alfa Laval AB, Tumba Sweden for support with computer resources.

Appendix

In this appendix we discuss the restrictions imposed by assuming that suspended droplets coalesce with the sediment–suspension interface, but not to any significant degree with each other in the interior of the suspension. Coalescence is to a large extent characterized by the finite contact time t_c required for a droplet to merge with a liquid–liquid interface, or two droplets to merge into a single drop. The contact time depends (among other things) on the force D that drives the droplet towards the interface (Liem & Woods 1974; Hartland & Vohra 1980).

For a suspended droplet that approaches a liquid–liquid interface (such as the surface of the sediment layer), t_c has been measured by, among others, Chen, Hahn & Slattery (1984). They gave an empirical correlation which can be used here to estimate the coalescence rate at the suspension–sediment interface. The drop–drop coalescence of small droplets in the interior of a sheared suspension seems to have been less studied. (The study of Ramamoorty & Treybal (1978) is not applicable here since the droplet Reynolds number was larger than unity, from 30 to 4000, there.)

As noted by Chen *et al.* (1984), the hydrodynamics of the approach of a drop to another drop show many similarities with the approach to a liquid interface. We will thus use their correlation to obtain an estimate of the coalescence rate in the bulk of the suspension. From dimensional arguments we estimate the force D between two drops that collide in the sheared suspension to be $D \simeq \mu a U_r$, where U_r is the relative velocity $(a/h)\,U \simeq (al/h^2)\,U_s$. Here U is the typical flow velocity, U_s is Stokes settling velocity (see 2.3), a is droplet radius, $2h$ channel width, l channel length and μ the viscosity. Two drops are assumed to coalesce only if they are in contact during a time longer than that given by t_c. Thus it is required that $t_c > h/U = h^2/(lU_s)$. Using the estimate of the interdrop force D derived above, substituted in the expression for t_c given by Chen *et al.*, we obtain the inequality on the right of the following two inequalities:

$$\frac{6}{c^{\frac{1}{3}}} \gg \left(\frac{\gamma a^3}{B}\right)^{\frac{1}{4}} \frac{\Delta\rho g a^2}{\gamma} \gg 2.45\frac{h^2}{al}. \tag{A 1}$$

Here γ is the surface tension, $\Delta\rho$ the density difference, c the volume fraction of droplets, $g = 9.81\ \mathrm{N/m^2}$ and $B = 10^{-28}\ \mathrm{Nm^2}$, a parameter characterizing the London–van der Waals forces.

The inequality to the left is derived from the requirement of a sufficiently rapid coalescence rate at the suspension–sediment interface. In order to have a sharp interface at the sediment surface, the number of droplets that can coalesce with the sediment per unit time and area must be larger than the number that are deposited on the interface. Otherwise a foam-like layer will appear instead of a liquid–liquid interface.

a, h and l in the right member of (A 1) are not independent. The requirement that a drop should be convected over a large part of the length of the channel before it reaches the lower plate ($\beta \simeq 1$) implies that $a^2 \sim (h^3/l)\,(3c/16)$. Using this, the right member becomes

$$2.45\frac{h^2}{al} = 2.45\left(\frac{h}{l}\right)^{\frac{1}{2}}\left(\frac{3c}{16}\right)^{-\frac{1}{2}}. \tag{A 2}$$

This is certainly smaller than the left-hand side of (A 1) for the slender vessels considered here, even for a volume fraction of order one. Thus the double inequality (A 1) is satisfied by a range of values of the parameters pertaining to surface tension and London–van der Waals forces in the middle member of (A 1).

REFERENCES

Acrivos, A. & Herbolzheimer, H. 1979 *J. Fluid. Mech.* **92**, 435.

Amberg, G., Dahlkild, A. A., Bark, F. H. & Henningson, D. S. 1986 *J. Fluid. Mech.* **166**, 473.

Batchelor, G. K. 1967 *An Introduction to Fluid Mechanics*. Cambridge University Press.

Boycott, A. E. 1920 *Nature* **104**, 532.

Chen, J.-D., Hahn, P. S. & Slattery, J. C. 1984 *AIChE J.* **30**, 622.

Davis, R. H. & Acrivos, A. 1985 *Ann. Rev. Fluid Mech.* **17**, 91.

Davis, R. H., Herbolzheimer, E. & Acrivos, A. 1982 *Intl J. Multiphase Flow* **8**, 571.

Engquist, B. & Osher, S. 1981 *Maths Comp.* **36**, 125.

Greenspan, H. P. & Ungarish, M. 1982 *Intl J. Multiphase Flow* **10**, 587.

Hartland, S. & Vohra, D. K. 1980 *J. Colloid Interface Sci.* **77**, 295.

Herbolzheimer, E. & Acrivos, A. 1981 *J. Fluid Mech.* **108**, 485.

Ishii, M. & Chawla, T. C. 1979 *Argonne Natl Lab. Rep.* ANL-79-105.

Kynch, G. J. 1952 *Trans. Faraday Soc.* **48**, 166.

Leung, W.-F. & Probstein, R. F. 1983 *I & EC Process Design & Develop.* **22**, 58.

Liem, A. J. S. & Woods, D. R. 1974 *Can. J. Chem. Engng* **52**, 222.

Probstein, R. F. & Hicks, R. E. 1978 *Ind. Water Engng* jan/feb.

Probstein, R. F., Yung, D. & Hicks, R. E. 1977 Paper presented at Theory, Practice and Process Principles for Physical Separation, Engng Foundation Conf., Asilomar, CA.

Ramamoorty, P. & Treybal, R. E. 1978 *AIChE J.* **24**, 985.

Roe, P. L. 1981 *J. Comp. Phys.* **43**, 357.

Richardson, J. F. & Zaki, W. N. 1954 *Trans. Instn Chem. Engrs* **32**, 35.

Rubinstein, R. 1980 *Intl J. Multiphase Flow*, **6**, 473.

Schneider, W. 1982 *J. Fluid Mech.* **120**, 323.